

New Approach for Evaluating Incomplete and Complete Fusion Cross Sections with Continuum-Discretized Coupled-Channels Method

Shintaro HASHIMOTO^{1,*}), Kazuyuki OGATA^{1,2}, Satoshi CHIBA^{1,3}, and Masanobu YAHIRO²

¹*Advanced Science Research Center, Japan Atomic Energy Agency, Ibaraki 319-1195, Japan*

²*Department of Physics, Kyushu University, Fukuoka 812-8581, Japan*

³*National Astronomical Observatory of Japan, Tokyo 181-8588, Japan*

We propose a new method for evaluating incomplete and complete fusion cross sections separately using the Continuum-Discretized Coupled-Channels method. This method is applied to analysis of the deuteron induced reaction on a ${}^7\text{Li}$ target up to 50 MeV of the deuteron incident energy. Effects of deuteron breakup on this reaction are explicitly taken into account. Results of the method are compared with those of the Glauber model, and the difference between the two is discussed. It is found that the energy dependence of the incomplete fusion cross sections obtained by the present calculation is almost the same as that obtained by the Glauber model, while for the complete fusion cross section, the two models give markedly different energy dependence. We show also that a prescription for evaluating incomplete fusion cross sections proposed in a previous study gives much smaller result than an experimental value.

The understanding of the fusion reaction mechanism is one of the most important and challenging subjects of nuclear physics. Description of *incomplete* fusion processes, in which a part of the projectile is absorbed by the target nucleus, with emitting other projectile fragment(s), is particularly interesting and important. So far, some theoretical models of the incomplete fusion, also called breakup fusion or inclusive breakup, of a two-body projectile have been proposed.¹⁾⁻³⁾ In these models, the incomplete fusion reaction was described as two-step processes, i.e., the projectile is broken up first and then one of the two constituents is absorbed by the target. The calculations of the fusion cross sections were carried out by using the Distorted Wave Born Approximation (DWBA) assuming that the emitted fragment can be treated as a spectator in the final state. Recently, roles of breakup (continuum) states of a weakly-bound projectile in the fusion reaction have been discussed^{4),5)} using the Continuum-Discretized Coupled-Channels method (CDCC).⁶⁾ CDCC was proposed and developed by Kyushu group, and has been successfully applied to analyze various reaction processes; see, e.g., Refs. 7)–9). In Ref. 4), an attempt to calculate the incomplete and complete fusion cross sections separately with CDCC was described. The assumption used in the separation of the two was, however, unrealistic for some reasons; we will return to this point later.

The incomplete fusion process in a deuteron induced reaction on Li targets at incident energies up to 50 MeV attracts wide interests of not only nuclear physicists but also nuclear engineers, because the emitted neutrons through this process

*) E-mail: hashimoto.shintaro@jaea.go.jp

are planning to be used in the International Fusion Materials Irradiation Facility (IFMIF).¹⁰⁾ Understanding of the reaction mechanism of this incomplete fusion process, or, equivalently, the inclusive (d, n) process, with evaluating theoretically the absolute value of the cross section is necessary. Moreover, nuclear data of inclusive (d, n) reactions on other various targets such as Be, Ta, and W are of crucial importance for studies on accelerator-based applications, i.e., shielding of the deuteron accelerators including IFMIF, and medical applications for Boron Neutron Capture Therapy (BNCT). Very recently, Ye *et al.*¹¹⁾ showed that the main part of the double differential cross section (DDX) data¹²⁾ of the emitted neutron from the inclusive ${}^7\text{Li}(d, n)$ reaction at 40 MeV is reproduced very well by the proton stripping cross section $d^2\sigma_{\text{STR}}^{(p)}/(dE_n d\Omega_n)$, which corresponds to the (d, n) incomplete fusion process in our terminology, added by the elastic breakup cross section $d^2\sigma_{\text{EB}}/(dE_n d\Omega_n)$; E_n and Ω_n are the energy and solid angle of the outgoing neutron. In their study, $d^2\sigma_{\text{STR}}^{(p)}/(dE_n d\Omega_n)$ and $d^2\sigma_{\text{EB}}/(dE_n d\Omega_n)$ are obtained by the Glauber model and CDCC, respectively, and the reason for the surprising success of the Glauber model at such low energies (~ 40 MeV) was discussed.¹¹⁾ Nevertheless, it is important to evaluate the accuracy of the Glauber model calculation of $d^2\sigma_{\text{STR}}^{(p)}/(dE_n d\Omega_n)$ below 40 MeV, in which experimental data are very scarce, by comparing it with that obtained fully quantum mechanically.

In this Letter, we propose a new approach for calculating the complete and incomplete fusion cross sections separately using CDCC. As an important advantage of the present method to the preceding studies,^{4), 13)} we separate the two fusion processes by the physics condition on the absorption of each constituent of the projectile by the target nucleus. In our model, a possible contribution of the breakup channels to the complete fusion process, as well as that of the elastic channel to the incomplete fusion process is properly taken into account. As we mention below, the new method contains a free parameter, i.e., the absorption radius. This parameter is determined using the result of the Glauber calculation at 40 MeV that can be interpreted as an experimental value of the proton-stripping incomplete fusion cross section. We then apply this method to the ${}^7\text{Li}(d, n)$ reactions at different deuteron incident energies from 10 MeV to 50 MeV. The (d, n) and (d, p) incomplete fusion cross sections and the complete fusion cross section thus evaluated are compared with the results^{11), 14)} obtained by the Glauber model. Note that we focus on the cross sections integrated over emission energies and angles in this work.

We describe the ${}^7\text{Li}(d, n)$ reaction with the three-body system shown in Fig. 1; \mathbf{R} is the relative coordinate between the ${}^7\text{Li}$ target and the center of mass of d , and \mathbf{r} is the relative coordinate between p and n . The coordinate of p (n) relative to ${}^7\text{Li}$ is denoted by \mathbf{r}_p (\mathbf{r}_n). The three-body Hamiltonian is given by

$$H = T_R + U_p(r_p) + U_n(r_n) + V^{\text{Coul}}(R) + T_r + V_{pn}(r), \quad (1)$$

where T_R and T_r represent the kinetic energy operators associated with \mathbf{R} and \mathbf{r} , respectively, U_p (U_n) is the optical potential between ${}^7\text{Li}$ and p (n), V^{Coul} is the Coulomb interaction between d and ${}^7\text{Li}$, and V_{pn} is the interaction between p and n . Note that we neglect the Coulomb breakup processes in this study, since we are

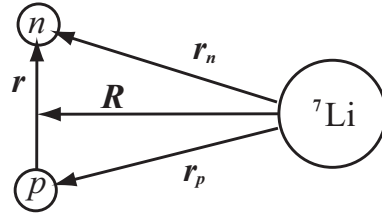


Fig. 1. Illustration of the three-body model of p , n and ${}^7\text{Li}$.

interested in the (d, n) reactions enough above the Coulomb barrier energy.

In CDCC, the three-body wave function $\Psi(\mathbf{R}, \mathbf{r})$ is expanded in terms of the eigenfunctions of the p - n system $\{\hat{\Phi}_i(\mathbf{r}), i = 0-i_{\max}\}$:

$$\Psi(\mathbf{R}, \mathbf{r}) = \sum_{JM} \sum_{i=0}^{i_{\max}} \left[\chi_i(\mathbf{R}) \otimes \hat{\Phi}_i(\mathbf{r}) \right]_{JM}, \quad (2)$$

where $\hat{\Phi}_0$ represents the ground state of d and $\hat{\Phi}_i$ ($i \neq 0$) the i th discretized continuum state. The *expansion coefficient* $\chi_i(\mathbf{R})$ describes the relative motion between d in the i th state and ${}^7\text{Li}$. The discretized continuum state $\hat{\Phi}_i$ is obtained by the so-called average method⁶⁾ as

$$\hat{\Phi}_i(\mathbf{r}) = \frac{1}{\sqrt{\Delta k_i}} \int_{k_{i-1}}^{k_i} dk \Phi(\mathbf{r}, k), \quad (3)$$

where $\Phi(\mathbf{r}, k)$ is the p - n scattering wave function with the relative wave number k , and $\Delta k_i = k_i - k_{i-1}$. $\Phi(\mathbf{r}, k)$ satisfies

$$[T_r + V_{pn}(r)] \Phi(\mathbf{r}, k) = \varepsilon \Phi(\mathbf{r}, k), \quad (4)$$

where $\varepsilon = \hbar^2 k^2 / (2\mu_r)$ with μ_r being the reduced mass of p and n .

The three-body Schrödinger equation using the wave function of Eq. (2) is given by

$$(H - E)\Psi(\mathbf{R}, \mathbf{r}) = 0, \quad (5)$$

where E is the total energy. Multiplying Eq. (5) by $\hat{\Phi}_j^*$ from the left, and integrating over \mathbf{r} , we obtain the following coupled-channel equations for $\chi_i(\mathbf{R})$:

$$\left(T_R + V_p^{\text{Coul}}(R) + \varepsilon_i - E \right) \chi_i(\mathbf{R}) = - \sum_j F_{ji}(\mathbf{R}) \chi_j(\mathbf{R}), \quad (6)$$

where ε_i is the internal energy of the p - n system in the i th state and

$$F_{ji}(\mathbf{R}) \equiv \langle \hat{\Phi}_j | (U_p + U_n) | \hat{\Phi}_i \rangle_{\mathbf{r}}$$

is the coupling form factor. Equations (6) are solved under the usual boundary conditions for $\chi_i(\mathbf{R})$.⁶⁾

The imaginary part of the optical potential is considered to describe the particle absorption by the target nucleus. Thus, the fusion cross section (absorption cross section) is given as the expectation value of the imaginary part with the wave function of the system. This cross section contains both contributions from the complete and incomplete fusion processes; we henceforth call this the total fusion cross section σ_{TF} . In the present three-body model calculation, σ_{TF} is obtained by

$$\sigma_{\text{TF}} = \frac{2\mu_R}{\hbar^2 K_0} |\langle \Psi | (-W_p - W_n) | \Psi \rangle|, \quad (7)$$

where W_p (W_n) is the imaginary part of U_p (U_n), μ_R is the reduced mass between d and ${}^7\text{Li}$, and K_0 is the d - ${}^7\text{Li}$ relative wave number in the incident channel. Note that the integrand on the right hand side (r.h.s.) of Eq. (7) is compact (L^2 integrable), since we discretize the p - n scattering wave functions with Eq. (3). Another important point to be noted is that the imaginary part of the nucleon- ${}^7\text{Li}$ optical potential describes not only nucleon absorption but also other processes such as the inelastic scattering to the excited states of ${}^7\text{Li}$. Since the nucleon absorption has the main contribution to the r.h.s. of Eq. (7), however, we regard it as the total ‘‘fusion’’ cross section as in many other studies on fusion reactions.

To separate the (d, p) and (d, n) incomplete fusion cross sections, $\sigma_{\text{IF}}^{(n)}$ and $\sigma_{\text{IF}}^{(p)}$ respectively, from σ_{TF} , we divide the integration region in Eq. (7) as follows. The explicit form of the expectation value on the r.h.s. of Eq. (7) is given by

$$|\langle \Psi | (-W_p - W_n) | \Psi \rangle| = - \int d\mathbf{r}_p \int d\mathbf{r}_n \Psi^*(\mathbf{R}, \mathbf{r}) \{W_p(\mathbf{r}_p) + W_n(\mathbf{r}_n)\} \Psi(\mathbf{R}, \mathbf{r}), \quad (8)$$

where we have changed the integration variables from (\mathbf{R}, \mathbf{r}) to $(\mathbf{r}_p, \mathbf{r}_n)$. We now separate the integration regions over r_p and r_n as

$$\begin{aligned} \int d\mathbf{r}_p \int d\mathbf{r}_n &= \int_{r_p < r_p^{\text{ab}}} d\mathbf{r}_p \int_{r_n < r_n^{\text{ab}}} d\mathbf{r}_n + \int_{r_p < r_p^{\text{ab}}} d\mathbf{r}_p \int_{r_n > r_n^{\text{ab}}} d\mathbf{r}_n \\ &+ \int_{r_p > r_p^{\text{ab}}} d\mathbf{r}_p \int_{r_n < r_n^{\text{ab}}} d\mathbf{r}_n + \int_{r_p > r_p^{\text{ab}}} d\mathbf{r}_p \int_{r_n > r_n^{\text{ab}}} d\mathbf{r}_n, \end{aligned} \quad (9)$$

where r_c^{ab} ($c = p$ or n) is the interaction range of W_c ; at $r_c > r_c^{\text{ab}}$, W_c is assumed to be negligible. The first term on the r.h.s. of Eq. (9) corresponds to the process in which both p and n are located within the range of W_c and absorbed by ${}^7\text{Li}$. In the second term, p is assumed to be within the range of the absorbing potential, while n is free of the absorption. Thus, it gives the integration region corresponding to the (d, n) incomplete fusion process. Similarly, the third term corresponds to the (d, p) incomplete fusion process. It is obvious from the definition of r_c^{ab} that the fourth term gives no contribution to σ_{TF} . Schematic illustration of these four integration regions is shown in Fig. 2. Using Eq. (9), σ_{TF} is decomposed into the complete fusion cross section σ_{CF} and the above-mentioned two incomplete fusion cross sections, i.e.,

$$\sigma_{\text{TF}} = \sigma_{\text{CF}} + \sigma_{\text{IF}}^{(p)} + \sigma_{\text{IF}}^{(n)}, \quad (10)$$

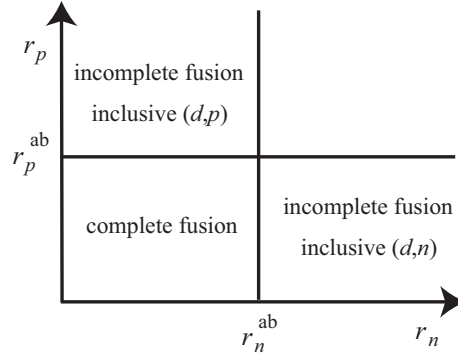


Fig. 2. Schematic illustration of the four integration regions. See text for details.

where

$$\sigma_{\text{CF}} = \frac{-2\mu_R}{\hbar^2 K_0} \int_{r_p < r_p^{\text{ab}}} d\mathbf{r}_p \int_{r_n < r_n^{\text{ab}}} d\mathbf{r}_n \bar{\Psi}^*(\mathbf{r}_p, \mathbf{r}_n) \{W_p(\mathbf{r}_p) + W_n(\mathbf{r}_n)\} \bar{\Psi}(\mathbf{r}_p, \mathbf{r}_n), \quad (11)$$

$$\sigma_{\text{IF}}^{(p)} = \frac{-2\mu_R}{\hbar^2 K_0} \int_{r_p < r_p^{\text{ab}}} d\mathbf{r}_p \int_{r_n > r_n^{\text{ab}}} d\mathbf{r}_n \bar{\Psi}^*(\mathbf{r}_p, \mathbf{r}_n) W_p(\mathbf{r}_p) \bar{\Psi}(\mathbf{r}_p, \mathbf{r}_n), \quad (12)$$

$$\sigma_{\text{IF}}^{(n)} = \frac{-2\mu_R}{\hbar^2 K_0} \int_{r_p > r_p^{\text{ab}}} d\mathbf{r}_p \int_{r_n < r_n^{\text{ab}}} d\mathbf{r}_n \bar{\Psi}^*(\mathbf{r}_p, \mathbf{r}_n) W_n(\mathbf{r}_n) \bar{\Psi}(\mathbf{r}_p, \mathbf{r}_n). \quad (13)$$

The total wave function $\bar{\Psi}(\mathbf{r}_p, \mathbf{r}_n)$ is obtained from $\Psi(\mathbf{R}, \mathbf{r})$, which is given by the CDCC calculation, by the straightforward transformation of the variables.

We remark here that the above expressions of the three components of the total fusion cross section are obtained by properly considering the physics condition on the absorption corresponding to each process as mentioned above. On the other hand, following the definition of the incomplete fusion cross sections of Refs. 4) and 13), $\sigma_{\text{IF}}^{(c)}$ ($c = p$ or n) could be expressed by

$$\sigma_{\text{IF,prev}}^{(c)} = \frac{-2\mu_R}{\hbar^2 K_0} \sum_{JM} \sum_{i \neq 0}^{i_{\text{max}}} \left\langle \left[\chi_i(\mathbf{R}) \otimes \hat{\Phi}_i(\mathbf{r}) \right]_{JM} \left| W_c \right| \left[\chi_i(\mathbf{R}) \otimes \hat{\Phi}_i(\mathbf{r}) \right]_{JM} \right\rangle, \quad (14)$$

i.e., the integration was done in the entire regions of (\mathbf{R}, \mathbf{r}) , with taking only the wave function in the breakup channels. The expression of Eq. (14) is unphysical, because (i) breakup channels can contribute not only the incomplete but also complete fusion processes, (ii) a possible contribution from the elastic channel is naively disregarded, and (iii) couplings between the channels of the three-body system, which have been included in the calculation of $\Psi(\mathbf{R}, \mathbf{r})$, are neglected in the evaluation of $\sigma_{\text{IF,prev}}^{(c)}$; the expression of the complete fusion given in Ref. 4), $\sigma_{\text{CF,prev}}$, has similar issues.

We apply the new method for calculating complete and incomplete fusion cross sections to the deuteron induced reactions on the ${}^7\text{Li}$ target for $10 \text{ MeV} \leq E_d^{\text{L}} \leq$

50 MeV, where E_d^L is the deuteron incident energy in the laboratory system. We use the CDCC codes CDCDEU and HICADEU¹⁵⁾ to obtain the CDCC wave function Ψ with assuming intrinsic spins of p , n , and ${}^7\text{Li}$ to be zero. As for V_{pn} , we adopt the Ohmura potential¹⁶⁾ that reproduces the deuteron energy in the ground state, i.e., $\varepsilon_0 = -2.23$ MeV. In the calculation of the p - n discretized continuum states, we include the s- and d-wave states; the maximum relative wave number k_{max} is determined by

$$k_{\text{max}} = \frac{1}{\hbar} \sqrt{2\mu_r(E_d^{\text{CM}} - |\varepsilon_0|)}$$

with E_d^{CM} being the d - ${}^7\text{Li}$ relative energy. The p - n continuum state is divided into 4 bin states, for each of the s- and d-waves. As for the p - ${}^7\text{Li}$ and n - ${}^7\text{Li}$ optical potentials, we use the parameter sets in Ref. 17) except that the spin-orbit terms are neglected in this study.

In the present formalism, the absorption radius r_c^{ab} is assumed to be a free parameter. In fact, it is found that the results of the incomplete fusion cross sections calculated with $r_c^{\text{ab}} = 4$ and 5 fm differ from each other by about 30%. Therefore, in this study, we determine r_c^{ab} at $E_d^L = 40$ MeV so that the $\sigma_{\text{IF}}^{(p)}$ agrees with the result of the Glauber model calculation; the latter, added by the elastic breakup contribution calculated with CDCC, reproduces the experimental DDX data very well at the same incident energy. The absorption radius thus determined is 4.0 fm, which is used for both p and n in all calculations in this study.

Figure 3 shows the results calculated with the new method; the dash-double-dotted, solid, dashed, and dash-dotted lines represent σ_{TF} , σ_{CF} , $\sigma_{\text{IF}}^{(p)}$, and $\sigma_{\text{IF}}^{(n)}$, respectively. One sees that σ_{CF} has the largest contribution to σ_{TF} in the energy region of our interest. Another important feature is that the energy dependence of $\sigma_{\text{IF}}^{(p)}$ is significantly different from that of $\sigma_{\text{IF}}^{(n)}$; at $E_d^L = 10$ MeV, $\sigma_{\text{IF}}^{(p)}$ is three times as large as $\sigma_{\text{IF}}^{(n)}$. This is due to the difference in the energy dependence of W_p and W_n ,

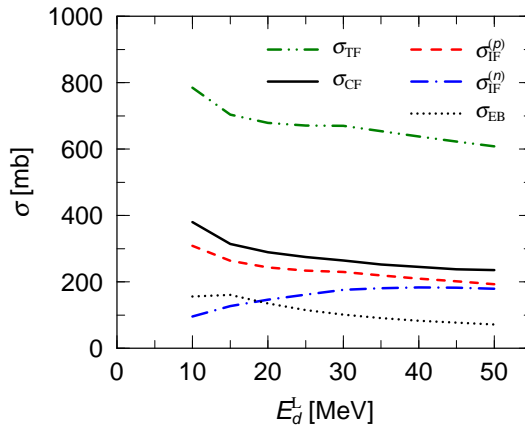


Fig. 3. (Color online) Results of σ_{TF} (dash-double-dotted line), σ_{CF} (solid line), $\sigma_{\text{IF}}^{(p)}$ (dashed line), and $\sigma_{\text{IF}}^{(n)}$ (dash-dotted line) for the deuteron induced reaction on ${}^7\text{Li}$ as a function of the incident energy E_d^L . The dotted line represents the elastic breakup cross sections calculated with CDCC.

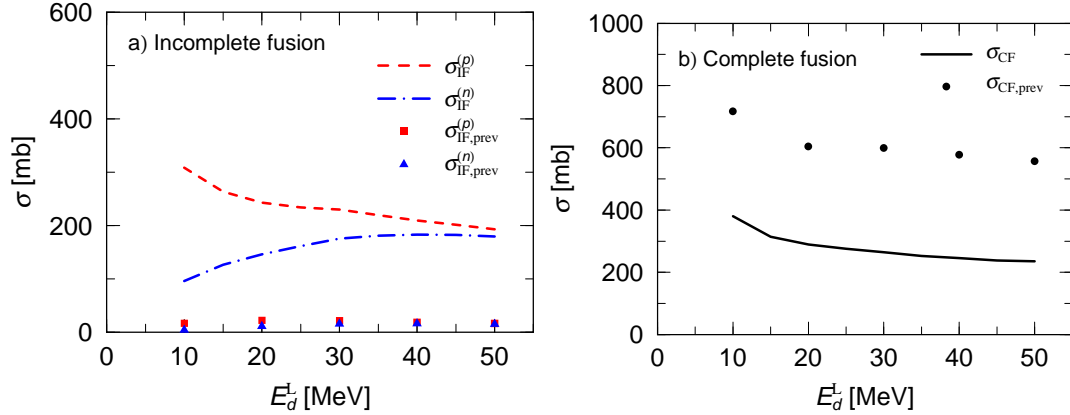


Fig. 4. (Color online) a) $\sigma_{\text{IF}}^{(p)}$ (dashed line) and $\sigma_{\text{IF}}^{(n)}$ (dash-dotted line) calculated with the present method, compared with $\sigma_{\text{IF,prev}}^{(p)}$ (squares) and $\sigma_{\text{IF,prev}}^{(n)}$ (triangles) following the previous definition given in Refs. 4) and 13). b) Comparison between the results of the complete fusion cross sections calculated with the present (solid line) and previous (dots) method.

i.e., W_p (W_n) at low energy is more (less) absorptive than that at around 40 MeV. The elastic breakup cross section σ_{EB} is also shown by the dotted-line in Fig. 3. The total neutron emission cross section, except for those by the compound and preequilibrium processes, can be evaluated as the sum of $\sigma_{\text{IF}}^{(p)}$ and σ_{EB} . It is found that contribution of σ_{EB} is much smaller than that of $\sigma_{\text{IF}}^{(p)}$, which is consistent with the conclusion of Ref. 11). On the other hand, if we consider the proton emission cross section below 20 MeV, which consists of $\sigma_{\text{IF}}^{(n)}$ and σ_{EB} , the two contributions are comparable.

Next we show in Fig. 4 the incomplete and complete fusion cross sections calculated with the previous expressions in Refs. 4) and 13), compared with the results of the present study. The squares and triangles in the left panel show, respectively, $\sigma_{\text{IF,prev}}^{(p)}$ and $\sigma_{\text{IF,prev}}^{(n)}$, and the dots in the right panel show $\sigma_{\text{CF,prev}}$. The lines shown in the panels are the same as in Fig. 3. One sees clearly that the previous prescription gives much smaller (larger) incomplete (complete) cross sections than those obtained by the present calculation. Our result of $\sigma_{\text{IF}}^{(p)}$ at 40 MeV, by definition, can be interpreted as an experimental value. Thus, the prescription given in Refs. 4) and 13) do not work at all at least for the inclusive ${}^7\text{Li}(d, n)$ reaction concerned. In other words, Fig. 4 clearly shows the importance of including elastic channel in the evaluation of $\sigma_{\text{IF}}^{(c)}$ ($c = p$ or n) as in Eqs. (12) and (13). Similarly, inclusion of the breakup channels in the calculation of σ_{CF} is also important.

As mentioned above, in Ref. 11), the contribution of the proton stripping process to the inclusive (d, n) cross section at 40 MeV was shown to be described very well by the Glauber model. It is thus interesting whether the Glauber model calculation works or not at even lower energies. For this purpose, in the left-upper panel in Fig. 5, we compare $\sigma_{\text{IF}}^{(p)}$ (short-dashed line) calculated with the present method, with $\sigma_{\text{STR}}^{(p)}$ (squares) obtained by the Glauber model calculation.¹¹⁾ Surprisingly,

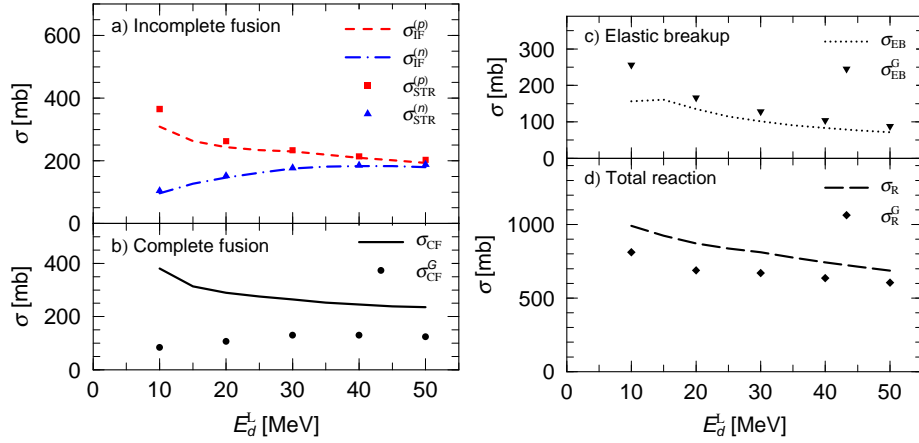


Fig. 5. (Color online) a) Comparison of $\sigma_{IF}^{(p)}$ (short-dashed line) and $\sigma_{IF}^{(n)}$ (dash-dotted line) obtained by the present calculation with $\sigma_{STR}^{(p)}$ (squares) and $\sigma_{STR}^{(n)}$ (triangles) by the Glauber model.¹¹⁾ b) Complete fusion cross sections calculated with the Glauber model (dots) and the present method (solid line). c) The elastic breakup cross section calculated with CDCC (dotted line) compared with that with the Glauber model (inverse triangles). d) The total reaction cross section obtained by CDCC (long-dashed line) is compared with that by the Glauber model (diamonds).

the two results agree well each other not only above 40 MeV but also at low energies down to 10 MeV. This is also the case with the neutron stripping process; one sees the good agreement between $\sigma_{IF}^{(n)}$ (dash-dotted line) and $\sigma_{STR}^{(n)}$ (triangles). Note that we use the absorption radius of 4.0 fm determined at 40 MeV in all the calculation as mentioned above. Thus, we conclude that the Glauber model calculation for the incomplete fusion cross sections is expected to work even at lower energies down to 10 MeV. On the other hand, as shown in the left-lower panel, the results of the complete fusion cross section σ_{CF}^G obtained by the Glauber model (dots)¹⁴⁾ significantly deviate from those obtained by the present study, i.e., σ_{CF} (solid line); even the energy dependence is different.

A possible reason for the success of the Glauber model in describing stripping processes is, as discussed in Ref. 11), that the contribution from the nuclear surface region is dominant, where the depth of the optical potential is so shallow that the Glauber model works well. On the other hand, since the complete fusion process takes place in the nuclear interior, the Glauber model does not work even at 50 MeV. It is numerically confirmed that when we make artificially the nucleon-⁷Li optical potential shallow, the difference shown in the left-lower panel becomes small, while the features of the incomplete fusion cross sections (left-upper panel) have no changes.

In the right-upper panel, we show the results of the elastic breakup cross section calculated with CDCC (dotted line) and the Glauber model (inverse triangles). The difference between the two is quite small above 10 MeV, which is found to be mainly due to the adiabatic approximation used in the Glauber model. The quite big difference at 10 MeV will come from the invalidity of the eikonal approximation also

assumed in the Glauber model. The total reaction cross section, which is the sum of the total fusion cross section and the elastic breakup one, calculated with CDCC (the Glauber model) is shown by the long-dashed line (diamonds) in the right-lower panel. The main part of the difference of the two comes from that in the complete fusion cross sections.

In summary, we propose a new method for evaluating the complete and incomplete fusion cross sections separately by means of CDCC. The separation of the two is carried out by the physics condition on the absorption for each fusion process. The absorption radius included in the present formalism is determined using the result of the proton stripping cross section for the ${}^7\text{Li}(d, n)$ reaction at 40 MeV calculated by the Glauber model, which was shown to reproduce the corresponding experimental value. The new method is applied to the ${}^7\text{Li}(d, n)$ reaction from 10 to 50 MeV. The complete fusion cross section is found to have the largest contribution to the total fusion cross section. The (d, p) and (d, n) incomplete fusion cross sections show quite different energy dependence, because of that in the imaginary parts of the p - ${}^7\text{Li}$ and n - ${}^7\text{Li}$ optical potentials. It is found that in the all energy region considered, the (d, p) and (d, n) incomplete fusion cross sections obtained by the Glauber model agree well with those obtained by the present calculation with CDCC. On the other hand, the two model calculations give significantly different results of the complete fusion cross section, even at 50 MeV. The complete and incomplete fusion cross sections obtained by the previous method of Refs. 4) and 13) are found to be inaccurate. Extension of the present framework to calculate the DDX is a very important future work. A method to divide the complete and incomplete processes unambiguously, i.e., without the absorption radius, will also be desirable.

We would like to thank Y. Watanabe and T. Ye for fruitful discussions and providing the numerical results. We also acknowledge helpful discussions with K. Hagino. SH thanks Y. Aoki for valuable discussions.

-
- 1) T. Udagawa and T. Tamura, Phys. Rev. C **24** (1981), 1348; Phys. Rev. C **33** (1986), 494.
 - 2) M. Ichimura, N. Austern, and C.M. Vincent, Phys. Rev. C **32** (1985), 432.
 - 3) M.S. Hussein and K.W. McVoy, Nucl. Phys. A **445** (1985), 124.
 - 4) A. Diaz-Torres and I.J. Thompson Phys. Rev. C **65** (2002), 024606.
 - 5) A. Diaz-Torres, I.J. Thompson, and C. Beck, Phys. Rev. C **68** (2003), 044607.
 - 6) M. Kamimura, M. Yahiro, Y. Iseri, Y. Sakuragi, H. Kameyama, and M. Kawai, Prog. Theor. Phys. Suppl. No. 89 (1986), 1.
N. Austern, Y. Iseri, M. Kamimura, M. Kawai, G. Rawitscher and M. Yahiro, Phys. Rep. **154** (1987), 125.
 - 7) K. Ogata, S. Hashimoto, Y. Iseri, M. Kamimura and M. Yahiro, Phys. Rev. C **73** (2006), 024605.
 - 8) T. Matsumoto, T. Egami, K. Ogata, Y. Iseri, M. Kamimura, and M. Yahiro, Phys. Rev. C **73** (2006), 051602(R).
 - 9) J. A. Tostevin, D. Bazin, B. A. Brown, T. Glasmacher, P. G. Hansen, V. Maddalena, A. Navin, and B. M. Sherrill, Phys. Rev. C **66** (2002), 024607.
A. M. Moro, R. Crespo, F. Nunes and I. J. Thompson, Phys. Rev. C **66** (2002), 024612.
 - 10) H. Matsui, in *Proceedings of the 23rd Symposium on Fusion Technology*, Venice, Italy, 20-24 Sept. (2004).
 - 11) T. Ye, Y. Watanabe, and K. Ogata, Phys. Rev. C **80** (2009), 014604.

- 12) M. Hagiwara, T. Itoga, N. Kawata, N. Hirabayashi, T. Oishi, T. Yamauchi, M. Baba, M. Sugimoto, and T. Muroga, *Fusion Sci. Technol.* **48** (2005) 1320.
- 13) M. Iijima, Y. Aoki, A. Ozawa, and N. Okumura, *Nucl. Phys. A* **793** (2007), 79.
- 14) T. Ye and Y. Watanabe (private communications).
- 15) Y. Iseri, M. Kamimura, M. Yahiro, Y. Sakuargi, and K. Ogata, *Bull. Res. Comput. Syst. Comput. Commun. Cent. Kyushu Univ.* Vol. 5, No. 3, 117 (2006) (CDCDEU); Vol. 1, No. 1, 16 (2007) (HICADEU).
- 16) T. Ohmura, B. Imanishi, M. Ichimura, and M. Kawai, *Prog. Theor. Phys.* **43** (1970), 347.
- 17) T. Ye, Y. Watanabe, K. Ogata, and S. Chiba, *Phys. Rev. C* **78** (2008), 024611.